# NMR · NQR and DTA · DSC Studies of Phase Transitions in Pyridinium Tetrachloropalladate(II) and Pyridinium Tetrachloroplatinate(II)*

Tetsuo Asaji, Keizo Horiuchi[a], Takehiko Chiba, Takashige Shimizu[b], and Ryuichi Ikeda[c]

Department of Chemistry, College of Humanities and Sciences, Nihon University, Sakurajosui, Setagaya-ku, Tokyo 156, Japan
[a] College of Science, University of the Ryukyus, 1 Senbaru, Nishihara, Okinawa 903-01, Japan
[b] Department of Chemistry, Faculty of Science, Nagoya University, Chikusa, Nagoya 464-01, Japan. Present address: Fuji Photo Film Co., Ltd.
[c] Department of Chemistry, University of Tsukuba, Tsukuba 305, Japan

Z. Naturforsch. **53a,** 419–426 (1998); received December 30, 1997

From the measurements of DTA · DSC and the temperature dependences of $^{35}$Cl NQR frequencies, phase transitions were detected at 150 K, 168 K, and 172 K for $(pyH)_2[PtCl_4]$, and at 241 K for $(pyH)_2[PdCl_4]$. In order to elucidate the motional state of the constituent ions in the crystals in connection with the structural phase transitions, the $^{35}$Cl NQR and $^1$H NMR spin-lattice relaxation times and the second moment of the $^1$H NMR line were measured as functions of temperature. For both compounds, the potential wells for the cationic reorientation are suggested to be highly nonequivalent at low temperatures. Above 168 K, the pyridinium ions in $(pyH)_2[PtCl_4]$ are expected to reorient between almost equivalent potential wells. As for $(pyH)_2[PdCl_4]$, it is expected that the orientational order of the cation still remains even above the second order transition at 241 K. A change of the potential curve from two-unequal to three-unequal wells is proposed as a possible mechanism of the second order transition. The activation energies for the cationic motion in the respective model potential are derived for both compounds at high and low temperatures.

*Key words:* Phase transition, NQR, NMR, Spin-lattice relaxation, DSC.

## 1. Introduction

Pyridinium compounds often show structural phase transitions. So far, phase transitions in pyridinium halides (pyH)X (X = Cl, Br, I) [1–4], pyridinium dichloroiodate(I) $(pyH)[ICl_2]$ [5], pyridinium tetrachloroiodate(III) $(pyH)[ICl_4]$ [6, 7], pyridinium hexafluorophosphate(V) $(pyH)[PF_6]$ [4], pyridinium hexahalometallates(IV) $(pyH)_2[MX_6]$ (M = Sn, Te, Pb; X = Cl, Br) [8–13], and pyridinium tetrahaloantimonates(III) $(pyH)[SbX_4]$ (X = Cl, Br) [14–16] have been studied by NMR, NQR and/or thermal measurements. These phase transitions are thought to be related to orientational order–disorder of the pyridinium ion in the crystals. In the present paper, we study phase transitions in pyridinium tetrachlorometallates(II) $(pyH)_2[MCl_4]$ (M = Pt, Pd) by measurements of the spin-lattice relaxation times of $^{35}$Cl NQR and $^1$H NMR, and the second moment of $^1$H NMR line as well as DTA and DSC measurements.

* Presented at the XIVth International Symposium on Nuclear Quadrupole Interactions, Pisa, Italy, July 20–25, 1997.

Reprint requests to Prof. T. Asaji; Fax: +81-3-53 17-94 33; e-mail: asaji@chs.nihon-u.ac.sp

## 2. Experimental

The samples were prepared according to the methods described in Gmelin's handbook [17, 18] or slight modifications of them. The preparation of $(pyH)_2[PtCl_4]$ by double decomposition of $K_2[PtCl_4]$ and (pyH)Cl was rather difficult since $K_2[PtCl_4]$ also tends to separate out. Elemental analysis (C, H, N, Cl) was made by the Elemental Analysis Center of Kyoto University. Calcd. for $(pyH)_2[PtCl_4]$: C, 24.2%; H, 2.43%; N, 5.64%; Cl, 28.5%. Found: C, 24.3%; H, 2.38%; N, 5.73%; Cl, 28.6%. Calcd. for $(pyH)_2[PdCl_4]$: C, 29.4%; H, 2.96%; N, 6.86%; Cl, 34.7%. Found: C, 30.2%; H, 2.93%; N, 7.00%; Cl, 34.2%.

X-Ray powder diffraction patterns were measured using Cu $K\alpha$ radiation employing a Rigaku RINT 2100S. Silicon powder was used as an internal standard for the diffraction angle. DTA measurements were made using a home-made apparatus with copper vs. constantan thermocouples. For DSC measurements, a differential scanning calorimeter DSC220 with a disk-station SSC5200 from Seiko Instruments Inc. was employed. NQR measurements were carried out by use of a pulsed Fourier transform spectrometer consisting of a Matec 515A gat-

0932-0784 / 98 / 0600-0419 $ 06.00 © – Verlag der Zeitschrift für Naturforschung, D-72027 Tübingen

Dieses Werk wurde im Jahr 2013 vom Verlag Zeitschrift für Naturforschung in Zusammenarbeit mit der Max-Planck-Gesellschaft zur Förderung der Wissenschaften e.V. digitalisiert und unter folgender Lizenz veröffentlicht: Creative Commons Namensnennung-Keine Bearbeitung 3.0 Deutschland Lizenz.

This work has been digitalized and published in 2013 by Verlag Zeitschrift für Naturforschung in cooperation with the Max Planck Society for the Advancement of Science under a Creative Commons Attribution-NoDerivs 3.0 Germany License.

Zum 01.01.2015 ist eine Anpassung der Lizenzbedingungen (Entfall der Creative Commons Lizenzbedingung „Keine Bearbeitung") beabsichtigt, um eine Nachnutzung auch im Rahmen zukünftiger wissenschaftlicher Nutzungsformen zu ermöglichen.

On 01.01.2015 it is planned to change the License Conditions (the removal of the Creative Commons License condition "no derivative works"). This is to allow reuse in the area of future scientific usage.

ed amplifier and an Iwatsu SM-2100 FFT signal analyzer. The $^{35}Cl$ NQR spin-lattice relaxation time $T_{1Q}$ was determined by the inversion recovery method observing the spin-echo signals. $^{1}H$ NMR spin-lattice relaxation times $T_1$ of $(pyH)_2[PtCl_4]$ and $(pyH)_2[PdCl_4]$ were determined by the saturation method at 30 MHz and the inversion recovery method at 16 and 20 MHz, respectively, by use of home-made pulsed NMR spectrometers. To determine the $^{1}H$ NMR second moment $M_2$, resonance absorptions were measured at ca. 14 MHz by means of a home-made Robinson-type spectrometer. The signals for several scans were averaged out by use of a digital stragescope Iwatsu DS-6612C. A correction for the finite modulation amplitude was made according to Andrew's equation [19].

In NQR, NMR, and DTA measurements, the samples were sealed in glass tubes with helium gas for heat exchange. The temperature was controlled and measured by use of copper vs. constantan and chromel vs. constantan thermocouples in the NQR and NMR measurements, respectively.

## 3. Results

### *3.1 X-Ray Powder Diffraction*

The diffraction patterns observed for the both compounds were very similar, suggesting that these two compounds are isomorphous. The lattice parameters were not determined due to the complexity of the patterns.

### *3.2 DTA and DSC*

Three endothermic anomalies were detected at 150, 168, and 172 K with increasing temperature in $(pyH)_2[PtCl_4]$. The phase transitions corresponding to these heat anomalies seem to be first order from the shape of DTA peaks and/or thermal hysterisis observed for the lowest-temperature one. The transition entropies were estimated as 0.6 and 9.4 J $K^{-1}$ $mol^{-1}$, respectively, for the 150 K and the successive (168 and 172 K) transitions from DSC measurements.

In $(pyH)_2[PdCl_4]$, a broad endothermic anomaly was observed at 241 K with increasing temperature, showing the occurrence of a second order phase transition. From the DSC measurements, the transition entropy was estimated as 4.4 J $K^{-1}$ $mol^{-1}$ for this transition. When the evacuation of $(pyH)_2[PdCl_4]$ is not complete before sealing in a glass tube, heat anomalies were observed above ca. 340 K, which may be due to a slight contamination by the very hygroscopic pyridinium chloride and/or decomposition. Pyridinium chloride could be eliminated by vacuum sublimation [2]. However, evacuation at elevated temperatures causes a decomposition. It was found that the crystals changed color and the new diffraction peaks grew in the X-ray powder pattern after several hours evacuation at 340–360 K.

### *3.3 $^{35}Cl$ NQR*

Two $^{35}Cl$ NQR frequencies were observed for $(pyH)_2[PtCl_4]$ and $(pyH)_2[PdCl_4]$. These frequencies were con-

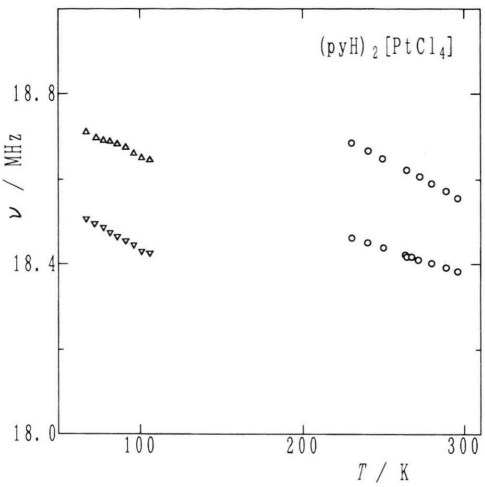


Fig. 1. Temperature dependences of the $^{35}Cl$ NQR frequencies of $(pyH)_2[PtCl_4]$.

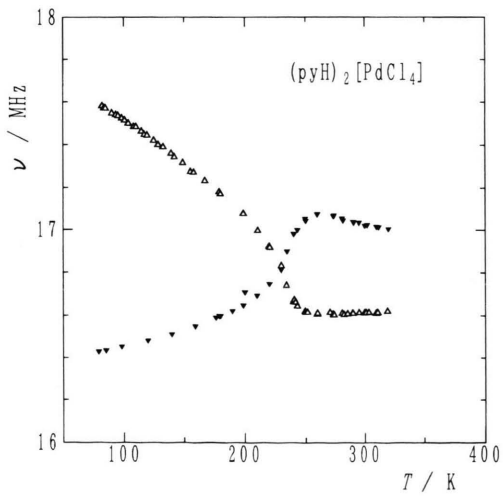


Fig. 2. Temperature dependences of the $^{35}Cl$ NQR frequencies of $(pyH)_2[PdCl_4]$.

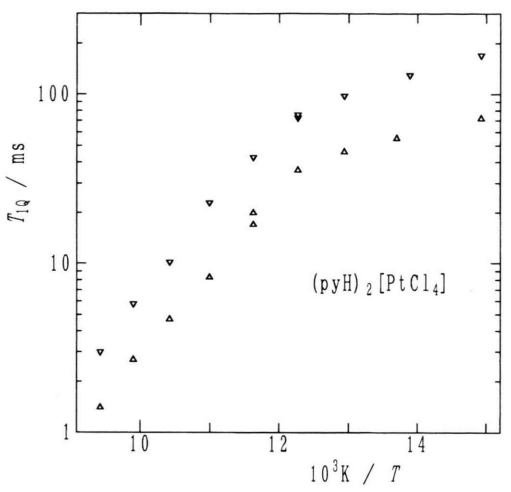


Fig. 3. Temperature dependences of the $^{35}$Cl NQR spin-lattice relaxation time $T_{1Q}$ of $(pyH)_2[PtCl_4]$. $T_{1Q}$ values are shown using the respective symbols for the different NQR lines as used in Figure 1.

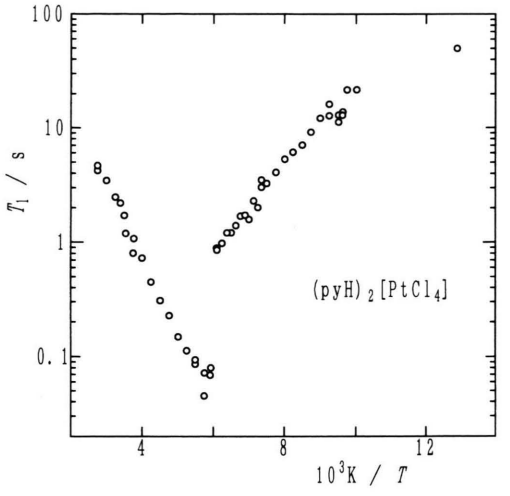


Fig. 5. Temperature dependences of the $^1$H NMR spin-lattice relaxation time $T_1$ of $(pyH)_2[PtCl_4]$, measured at 30 MHz.

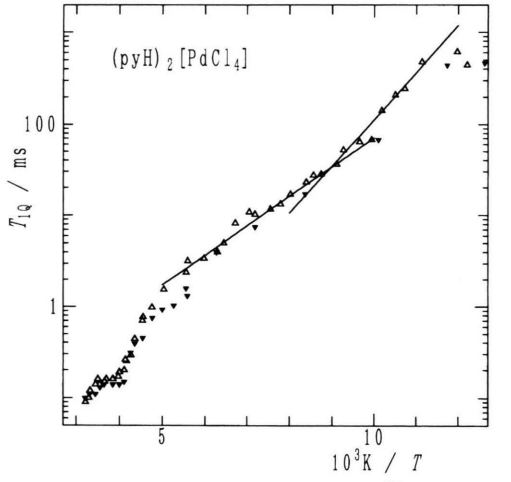


Fig. 4. Temperature dependences of the $^{35}$Cl NQR spin-lattice relaxation time $T_{1Q}$ of $(pyH)_2[PdCl_4]$. $T_{1Q}$ values are shown using the respective symbols for the different NQR lines as used in Figure 2. The solid lines are fittings by the equations (18) and (21) (see text).

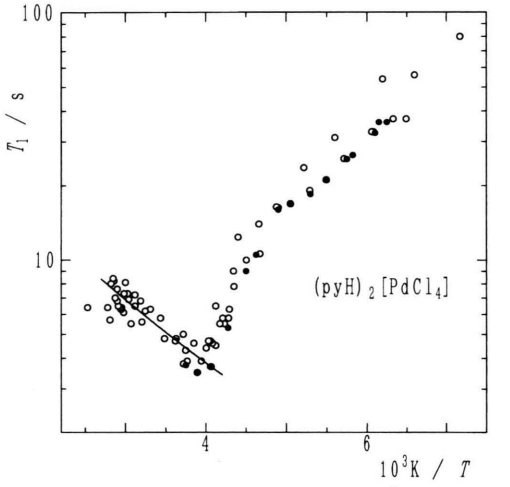


Fig. 6. Temperature dependences of the $^1$H NMR spin-lattice relaxation time $T_1$ of $(pyH)_2[PdCl_4]$, measured at 16 MHz (●) and 20 MHz (○). The solid curve indicates the least-square-fitting by use of (10) with $\Delta E = 3.8$ kJ mol$^{-1}$ (see text).

sistent with the reported values of 18.41 and 18.60 MHz for $(pyH)_2[PtCl_4]$, and 16.61 and 17.08 MHz for $(pyH)_2[PdCl_4]$ at 273 K [20]. The temperature dependences of the NQR frequencies are depicted in Figs. 1 and 2 for $(pyH)_2[PtCl_4]$ and $(pyH)_2[PdCl_4]$, respectively. The temperature dependences of $T_{1Q}$ are shown in Figs. 3 and 4 for $(pyH)_2[PtCl_4]$ and $(pyH)_2[PdCl_4]$, respectively. In the temperature range of 110–220 K, the NQR signals of $(pyH)_2[PtCl_4]$ could hardly be detected. For $(pyH)_2[PdCl_4]$, a discontinuous change in the slope of the frequency shift as a function of temperature was observed at 245 K. $T_{1Q}$ of $(pyH)_2[PtCl_4]$ was shortend above ca. 80 K with increasing temperature, following an exponential law. $T_{1Q}$ of $(pyH)_2[PdCl_4]$ decreased also rather rapidly compared with the temperature dependence $T_{1Q} = aT^{-2}$, which is expected for the lattice vibra-

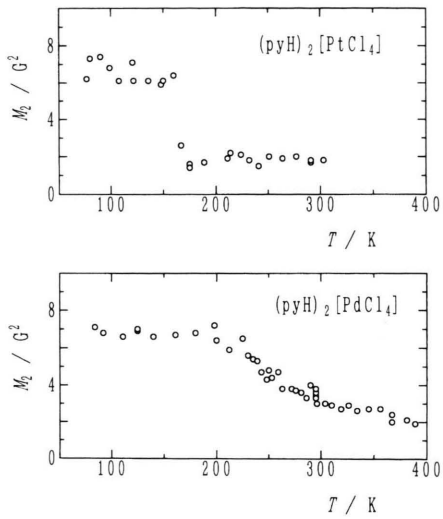


Fig. 7. Temperature dependences of the $^1$H NMR second moment $M_2$ for $(pyH)_2[PtCl_4]$ and $(pyH)_2[PdCl_4]$.

tional mechanism. By fitting the $T_{1Q}$ data below 230 K to $T_{1Q}=aT^{-n}$, $n$=ca. 7 was obtained.

### *3.4 $^1$H NMR*

The temperature dependences of $T_1$ of $(pyH)_2[PtCl_4]$ and $(pyH)_2[PdCl_4]$ are shown in Figs. 5 and 6, respectively. $T_1$ of $(pyH)_2[PtCl_4]$ showed a discontinuous change at ca. 167 K. $T_1$ of $(pyH)_2[PdCl_4]$ was quite long and very weakly Larmor-frequency dependent below 270 K. A cusp was observed at around 250 K. The temperature dependences of $M_2$ of both compounds are shown in Figure 7. An abrupt decrease of $M_2$ was observed at around 170 K with increasing temperature in $(pyH)_2[PtCl_4]$, while a gradual decrease of $M_2$ from ca. 7 G$^2$ at around 200 K to ca. 2 G$^2$ at around 400 K was observed in $(pyH)_2[PdCl_4]$.

## 4. Discussion

### *4.1 $(pyH)_2[PtCl_4]$*

In the temperature range of 110–220 K, where the NQR signals were unobservable, three thermal anomalies were detected at 150, 168, and 172 K in the DTA measurements. Therefore, the disappearance will be connected with structural phase transitions. Above the transition temperature $T_c$=168 K, the $^1$H NMR $M_2$ decreases abruptly to ca. $\frac{2}{7}$ of the lowest-temperature value, as shown in Figure 7. This suggests that a motion of the pyridinium cation is excited. By assuming a 60° two-site jump of the pyridinium cation around its pseudo $C_6$ axis and taking only the intramolecular contributions into account, one finds that the ratio $R$ of the motionally averaged $M_2$ to the rigid lattice one decreases to $\frac{7}{16}$ [12], which value is larger than the observed value of ca. $\frac{2}{7}$. Therefore, the motion of the pyridinium cation in the high-temperature phase is expected to take place between more than two sites. The discontinuous change of the $^1$H NMR $T_1$ at $T_c$=168 K, associated with the change in the sign of $dT_1/d(1/T)$, indicates the correlation time of the motion jumps at the transition. From the temperature coefficient, the apparent activation energies of the motion were estimated as 13.7 and 7.7 kJ mol$^{-1}$ for above and below 168 K, respectively. The activation energy of 13.7 kJ mol$^{-1}$ may be assigned to the motion between more than two sites. These sites are expected to be almost equivalent above 168 K, since a constant low $M_2$ value was observed above this temperature. A lower activation energy was obtained for the low-temperature phases. The transition at 168 K is expected to be of the order–disorder type, judging from the large entropy change observed. Hence, it is reasonable to assume nonequivalent potential wells for the cationic motion in the low-temperature phases. The reason for the lower value at lower temperatures may be attributed to the inequivalence of the potential wells. This is because, when the potential wells for the motion are highly nonequivalent, the slope of $\ln T_1$ vs. $1/T$ does not always give the activation energy required to overcome the barrier [3, 13, 21]. That is, the apparent value does not correspond to the true barrier height for the motion. At the $T_c$=150 K transition with $\Delta S_{tr}$=0.6 J K$^{-1}$ mol$^{-1}$, no anomaly was observed in the temperature dependences of $^1$H $M_2$, $T_1$ showing little change of motional state of the cation.

Now, let us turn to the origin of the exponential decrease of $T_{1Q}$ observed above ca. 80 K. The activation energies estimated from the slopes of $\ln T_{1Q}$ vs. $1/T$ for the high- and low-frequency lines are 10 and 11 kJ mol$^{-1}$, respectively. These values are comparable to the observed value of 7.7 kJ mol$^{-1}$ for the cationic motion in the low-temperature phases. From this, it is likely that the quadrupolar relaxation is also caused by the cationic motion. The EFG produced by the surrounding cations at the resonant nucleus will fluctuate due to the cationic motion, providing an effective mechanism for the spin-lattice relaxation [13]. Since the magnitude of the modulation will differ from site to site, the finding that the crystallographically nonequivalent chlorines have differ-

ent $T_{1Q}$ values can be explained by assuming this mechanism. On the other hand, if the $T_{1Q}$ decrease is due to the reorientational motion of the complex anion $[PtCl_4]^{2-}$ itself, the chlorine within the same complex anion should have the same $T_{1Q}$ value. Therefore, in order to explain the $T_{1Q}$ results by the anionic reorientation, we have to assume two crystallographically nonequivalent complex anions having four equivalent chlorines each. However, it is not likely that the anion retains a strictly square planar structure in such a low-symmetry crystal which shows very many lines in the X-ray powder diffraction.

If the exponential decrease of $T_{1Q}$ can be ascribed to the EFG-modulation by the cationic motion, the activation energies derived from the temperature dependence of $T_{1Q}$ and $^1H$ $T_1$ should coincide in the same temperature range. Unfortunately, at $10^3$ K/$T$ > 10 the lattice vibrational contribution to the $^1H$ $T_1$ seems to become significant. On the other hand, $T_{1Q}$ could be determined only at $10^3$ K/$T$ > 9.5. Therefore, the activation energies of ca. 8 and 10 kJ mol$^{-1}$ were derived from $T_1$ and $T_{1Q}$ for the temperature range of $10^3$ K/$T$ < 10 and $10^3$ K/$T$ > 10, respectively. These values can not be directly compared with each other since they were estimated in different temperature ranges. As will be described later in the discussion of $(pyH)_2[PdCl_4]$, when the cation reorients between nonequivalent sites, the activation energies determined from $T_1$ at $10^3$ K/$T$ < 10 and from $T_{1Q}$ at $10^3$ K/$T$ > 10 may be assigned to $-(E_A-2\Delta E)$ and $E_A$, respectively, providing the cationic motion is fast and slow in the respective temperature range. Here, $E_A$ is the activation energy for the transition from the deep to the shallow well, and $\Delta E$ is the energy difference between the unequal wells. We can not say from the present results, whether the unequal potential wells consist of two or three minima. Putting $-(E_A-2\Delta E)=8$ kJ mol$^{-1}$ and $E_A=10$ kJ mol$^{-1}$, $\Delta E=9$ kJ mol$^{-1}$ is obtained.

### 4.2 *(pyH)$_2$[PdCl$_4$]*

The phase transition at $T_c=241$ K can be classified to the second order because the peak temperatures of very broad heat anomalies observed with increasing and decreasing temperature almost coincide, and the NQR frequencies change continuously through $T_c$. In contrast to $(pyH)_2[PtCl_4]$, $^1H$ $M_2$ shows a very gradual smooth decrease with increasing temperature, as shown in Figure 7. No remarkable anomaly was observed at the temperature where the heat anomaly was detected. A gradual $M_2$ decrease over such a wide temperature range is expected to occur in case of highly nonequivalent potential wells [21, 22] since, if a molecular motion occurs between nonequivalent sites, the temperature dependence curve of $M_2$ becomes a function of the parameter which represents the population ratio between nonequivalent sites. If a change of the potential wells such as from nonequivalent to equivalent is associated with a phase transition, a remarkable decrease in $M_2$ will take place at the transition. The small change of $M_2$ at the transition temperature suggests that the inequivalence of potential wells remains above the transition. The transition entropy of the phase transition at $T_c=241$ K was estimated to be $\Delta S_{tr}=4.4$ J K$^{-1}$ mol$^{-1}$, which is much smaller than the entropy change expected for, e.g., the doubling of the number of sites ($2R\ln 2=11.6$ J K$^{-1}$ mol$^{-1}$). This suggests that the orientational order of the pyridinium cation still remains above 241 K, supporting the above expectation.

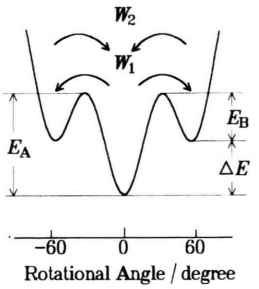


Fig. 8. Unequal-three-well potential for the cationic motion in $(pyH)_2[PdCl_4]$ above 241 K.

Because $M_2$ decreases to ca. $\frac{2}{7}$ of the low-temperature plateau value, it is expected that the cation reorients between more than two sites above 241 K. We, therefore, propose a three-well-potential having one deeper well as shown in Fig. 8 for the cationic motion. For the motion in this model potential, the temperature dependence of the ratio $R(T)$ of the motionally averaged $M_2$ to the rigid lattice one, taking only the intramolecular contribution into account [22], is given by

$$R(T)=\frac{\langle M_2^{\text{motion}}\rangle_p}{\langle M_2^{\text{rigid}}\rangle_p}=\left(\frac{a-1}{a+2}\right)^2+\frac{3}{4}\frac{(2a+1)}{(a+2)^2}. \qquad (1)$$

Here, $\langle\ \rangle_p$ denotes the powder average for a polycrystalline sample and, using the energy difference $\Delta E$ between the deep and the shallow wells, a population parameter $a$ is defined by

$$a=\exp(\Delta E/RT). \qquad (2)$$

$R(T)$ in the range of 260–340 K was least-square-fitted by use of (1). $\Delta E = 3.8$ kJ mol$^{-1}$ was obtained by the fitting calculations, as shown in Figure 9. The deviation of the observed $R(T)$ from the fitting curve beyond the above temperature range shows that $\Delta E$ is no more considered to be a constant parameter over the wide temperature range. The deviation in the low-temperature phase may be ascribed to the change of potential shape associated with the structural phase transition. In the low-temperature phase, it is expected from the shift of the NQR frequencies depicted in Fig. 2 that the hydrogen-bonding between the cation and the chlorine changes with decreasing temperature. We tentatively propose the following model: Above $T_c = 241$ K, the cation forms a bifurcated hydrogen-bond with the two chlorines Cl(1) and Cl(2) within the $[PdCl_4]^{2-}$ complex anion when the N–H bond orients parallel to the bisector of the angle Cl(1)–Pd–Cl(2) as shown in Figure 10. Then we may have to take additionally the two orientations obtained by ±60° rotation of the cation about its pseudo $C_6$ axis into account as metastable orientations to get a three-well-potential model. With decreasing temperature through $T_c$, a displacive rotation of the cation and/or anion may take place. Then the cation may form hydrogen-bonds at the two cationic orientations, as shown in Fig. 10 for a plausible arrangement. In this situation, it may be reasonable to take only the two orientations which are related by the ±60° rotation into account.

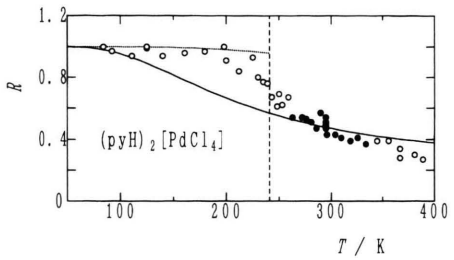


Fig. 9. Temperature dependence of the normalized second moment $R$ for $(pyH)_2[PdCl_4]$. The vertical broken line denotes the transition temperature of 241 K. The solid curve indicates the least-squares-fitting for 260–340 K by use of the unequal-three-well potential of Fig. 8 with $\Delta E = 3.8$ kJ mol$^{-1}$. The data points used for the calculation are indicated by solid circles. The dotted curve is calculated by use of the unequal-two-site model of Fig. 11 with $\Delta E = 8$ kJ mol$^{-1}$ ((22) in the text).

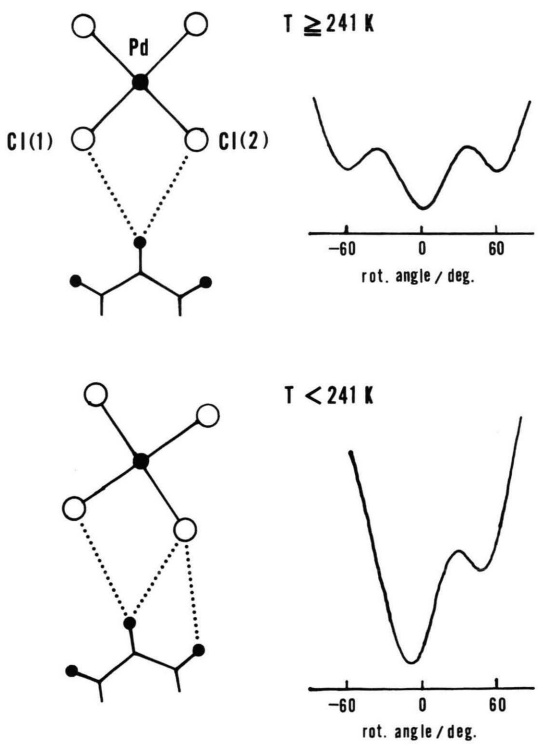


Fig. 10. The plausible interionic interactions and the potential curves for the cationic motion in $(pyH)_2[PdCl_4]$ are schematically shown for above and below 241 K.

Assuming the three-well-potential model, we have analyzed the $^1$H $T_1$ data in the temperature range of ca. 250–340 K. The intramolecular contribution to the spin-lattice relaxation rate $T_1^{-1}$ due to the reorientational motion between the three potential minima shown in Fig. 8 is given by [21, 22]

$$T_1^{-1} = \gamma^2 (\Delta M_2)_{\text{intra}} \cdot \left[ \frac{3a}{(a+2)^2} B(\tau_{c1}) + \frac{1}{(a+2)} B(\tau_{c2}) \right]. \quad (3)$$

Here, $\gamma$ is the gyromagnetic ratio of a proton, $(\Delta M_2)_{\text{intra}}$ is the $M_2$ difference of the intramolecular contributions between the rigid lattice value and the motionally narrowed one at high enough temperature. Other symbols are expressed as

$$a = \exp(\Delta E / RT), \quad (4)$$

$$B(\tau_c) = \frac{\tau_c}{1 + \omega_0^2 \tau_c^2} + \frac{4\tau_c}{1 + 4\omega_0^2 \tau_c^2}. \quad (5)$$

The correlation times $\tau_{c1}$ and $\tau_{c2}$ of the motional process in question are written by use of the transition probability rates $W_1$ and $W_2$ from deep to shallow minimum and vice versa, respectively, as

$$\tau_{c1} = (2W_1 + W_2)^{-1}, \quad (6)$$

$$\tau_{c2} = W_2^{-1}. \quad (7)$$

$W_1$ and $W_2$ can be written by

$$W_1 = K \exp(-E_A/RT)\,, \tag{8}$$

$$W_2 = K \exp(-E_B/RT)\,, \tag{9}$$

where $K$ is a jumping frequency factor and $E_A$ and $E_B$ are activation energies for jumps from deep to shallow minimum and vice versa, respectively. For the fast motion limit of $\omega_0^2 \tau_c^2 \ll 1$, $B(\tau_c)$ approximates to $5\tau_c$, and then

$$T_1 = C \frac{(a+2)^3}{(a^2+a+1)} \exp(-E_B/RT) \tag{10}$$

is obtained for the spin-lattice relaxation time. Here $C$ is given by

$$C = \left(\frac{1}{20}\right) \gamma^{-2} (\Delta M_2)_{\text{intra}}^{-1} K\,. \tag{11}$$

By use of (10) with the fixed $\Delta E$ value of 3.8 kJ mol$^{-1}$ derived from the $M_2$ variation with temperature, we have performed the least-square fitting calculations to obtain $C = 6.46 \pm 0.08$ s and $E_B = 6.3$ kJ mol$^{-1}$. By the foregoing analysis, the parameters which describe the potential curve for the motion in the high-temperature phase were obtained as $E_A = 10.1$ kJ mol$^{-1}$, $E_B = 6.3$ kJ mol$^{-1}$, and $\Delta E = 3.8$ kJ mol$^{-1}$.

To estimate the potential curve for the low-temperature phase below 241 K, the temperature dependence of $T_{1Q}$ in the temperature range of 90–200 K was analyzed by assuming a two-site jump of the pyridinium cation between unequal potential wells and the spin-lattice relaxation mechanism due to the modulation of the EFG by the cationic motion [13]. This relaxation rate can be written as

$$T_{1Q}^{-1} = \frac{1}{12}\left(\frac{e^2 Qq}{\hbar}\right)^2 \frac{4a}{(1+a)^2}\left(\frac{q'}{q}\right)^2 \frac{\tau_c}{(1+\omega_Q^2 \tau_c^2)}\,, \tag{12}$$

where $e^2Qq/\hbar$, $\omega_Q$, $q'/q$, and $\tau_c$ denote the quadrupole coupling constant, the nuclear quadrupole angular frequency of chlorine, the fluctuation fraction of the field gradient, and the correlation time of the cationic motion, respectively. The population parameter $a$ is defined for the unequal-two-well potential of Fig. 11 as

$$a = \exp(\Delta E/RT)\,. \tag{13}$$

The correlation time $\tau_c$ is written by use of the transition probability rates $W_1$ and $W_2$ from deep to shallow minimum and vice versa, respectively, as

$$\tau_c = (W_1 + W_2)^{-1}\,. \tag{14}$$

For the transition probability rate, the Arrhenius relation can again be assumed (cf. (8), (9)).

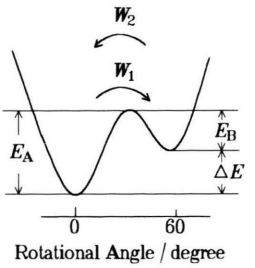


Fig. 11. Unequal-two-well potential for the cationic motion in $(pyH)_2[PdCl_4]$ below 241 K.

When the cationic motion is so fast that $\omega_Q^2 \tau_c^2 \ll 1$, (12) is reduced to

$$T_{1Q}^{-1} = C_q \frac{4a}{(1+a)^2} \tau_c\,, \tag{15}$$

with

$$C_q = \frac{1}{12}\left(\frac{e^2 Qq}{\hbar}\right)^2 \left(\frac{q'}{q}\right)^2\,. \tag{16}$$

From (14) in (15) follows

$$T_{1Q}^{-1} = C_q K^{-1} \frac{4a}{(1+a)^3} \exp(E_A/RT)\,. \tag{17}$$

For $a \gg 1$

$$T_{1Q}^{-1} = 4 C_q K^{-1} \exp[(E_A - 2\Delta E)/RT]\,. \tag{18}$$

Therefore, the slope of $\ln T_{1Q}$ vs. $1/T$ gives the value of $-(E_A - 2\Delta E)/R$. If $2\Delta E > E_A$, then the slope becomes positive even when the fast motion limit is applicable. At the slow motion limit $\omega_Q^2 \tau_c^2 \gg 1$ we have

$$T_{1Q}^{-1} = \frac{C_q}{\omega_Q^2} \frac{4a}{(1+a)^2} \tau_c^{-1}\,. \tag{19}$$

Putting (14) into (19)

$$T_{1Q}^{-1} = \frac{C_q}{\omega_Q^2} K \frac{4a}{(1+a)} \exp(-E_A/RT)\,. \tag{20}$$

If $a \gg 1$,

$$T_{1Q}^{-1} = 4 C_q K \omega_Q^{-2} \exp(-E_A/RT)\,. \tag{21}$$

Therefore, at low-enough temperatures the slope of $\ln T_{1Q}$ vs. $1/T$ gives the value of $E_A/R$.

Looking at the temperature dependence of $T_{1Q}$ in the temperature range of 90–200 K ($5 \leq 10^3$ K$/T \leq 11$), we devided the curve at around $10^3$ K$/T = 9$ into two approx-

imately linear parts, as shown in Figure 4. From the respective linear parts for $10^3\ \mathrm{K}/T < 9$ and $9 < 10^3\ \mathrm{K}/T$, $-(E_A - 2\Delta E)/R$ and $E_A/R$ were determined to be $0.74 \times 10^3$ K and $1.18 \times 10^3$ K, respectively. That is, for the low-temperature phase $E_A = 9.8$ kJ mol$^{-1}$, $E_B = 1.8$ kJ mol$^{-1}$, and $\Delta E = 8$ kJ mol$^{-1}$, assuming the potential curve shown in Figure 11. The energy difference between unequal potential wells is quite large, so $a \gg 1$ is well satisfied up to 200 K. By use of $\Delta E = 8$ kJ mol$^{-1}$ we have calculated the temperature dependence of the normalized second moment $R(T)$ as indicated by the dotted curve in Figure 9. For the 60° two-site jump model between the unequal potential wells of Fig. 11,

$$R(T) = \frac{\langle M_2^{\mathrm{motion}} \rangle_p}{\langle M_2^{\mathrm{rigid}} \rangle_p} = \frac{a^2 - a/4 + 1}{(1+a)^2}, \qquad (22)$$

where only the intramolecular contribution was taken into account. Above 200 K, the deviation from the calculated curve becomes significant, showing that a deformation of the potential curve is going on when $T$ approaches $T_c = 241$ K from below.

## 5. Conclusions

1. $(pyH)_2[PtCl_4]$ undergoes phase transitions at 150, 168, and 172 K. The 168 K transition is of the order–disorder type with the pyridinium orientation.

2. Above 168 K, the pyridinium ions are expected to reorient between almost equivalent potential wells. The activation energy for the motion was estimated to be about 14 kJ mol$^{-1}$.

3. The potential wells below 168 K could be highly nonequivalent. Using the two- or three-well model, we obtained $E_A = 10$ kJ mol$^{-1}$ and $E_B = 1$ kJ mol$^{-1}$ for the activation energies.

4. $(pyH)_2[PdCl_4]$ undergoes a second order phase transition at 241 K. The orientational order of the cation still remains above the second order transition.

5. It is proposed that the displacive rotation of the cation and/or anion is connected to the second order transition. Unequal two- and three-well potentials are proposed for the phases below and above 241 K, respectively.

6. The activation energies for the cationic motion between the unequal two potential-wells below 241 K are estimated as $E_A = 10$ kJ mol$^{-1}$ and $E_B = 2$ kJ mol$^{-1}$. Those between the unequal three potential-wells above 241 K are estimated as $E_A = 10$ kJ mol$^{-1}$ and $E_B = 6$ kJ mol$^{-1}$.

*Acknowledgements*

Mr. T. Yogo and Mr. S. Ohta (Nihon University), and Ms. Y. Ito-Kawamoto (Nagoya University) are greatly acknowledged for sample preparations and/or collaboration in the measurements. Thanks are also due to Dr. H. Fujimori and Mr. T. Ishizaka (Nihon University) for the characterization of $(pyH)_2[PdCl_4]$.

[1] C. H. Matthews and D. F. R. Gilson, Can. J. Chem. **48,** 2625 (1970).
[2] J. A. Ripmeester, Can. J. Chem. **54,** 3453 (1976).
[3] J. A. Ripmeester, J. Chem. Phys. **85,** 747 (1986).
[4] M. Hanaya, N.Ohta, and M. Oguni, J. Phys. Chem. Solids **54,** 263 (1993).
[5] R. Watanabe, T. Asaji, Y. Furukawa, D. Nakamura, and R. Ikeda, Z. Naturforsch. **44a,** 1111 (1989).
[6] K. B. Dillon and T. C. Waddington, Inorg. Nucl. Chem. Lett. **14,** 415 (1978).
[7] A. Ishikawa, T. Asaji, and D. Nakamura, Z. Naturforsch. **44a,** 1226 (1989).
[8] K. B. Dillon, J. Halfpenny, and A. Marshall, J. Chem. Soc. Dalton Trans. **1985,** 1399.
[9] D. Borchers and Al. Weiss, Z. Naturforsch. **42a,** 739 (1987).
[10] Y. Ito, T. Asaji, and D. Nakamura, Phys. Stat. Sol. (a) **104,** K97 (1987).
[11] Y. Tai, A. Ishikawa, K. Horiuchi, T. Asaji, D. Nakamura, and R. Ikeda, Z. Naturforsch. **43a,** 1002 (1988).
[12] Y. Tai, T. Asaji, R. Ikeda, and D. Nakamura, Z. Naturforsch. **44a,** 300 (1989).
[13] Y. Tai, T. Asaji, D. Nakamura, and R. Ikeda, Z. Naturforsch. **45a,** 477 (1990).
[14] T. Okuda, K. Yamada, H. Ishihara, M. Hiura, S. Gima, and H. Negita, Chem. Soc. Chem. Commun. **1981,** 979.
[15] T. Okuda, Y. Aihara, N. Tanaka, K. Yamada, and S. Ichiba, J. Chem. Soc. Dalton Trans. **1989,** 631.
[16] K. Yamada, T. Ohtani, S. Shirakawa, H. Ohki, T. Okuda, T. Kamiyama, and K. Oikawa, Z. Naturforsch. **51a,** 739 (1996).
[17] Gmelins Handbuch der Anorganischen Chemie, **Pt(68),** Teil C2, 226, Verlag Chemie, Berlin 1957.
[18] Gmelins Handbuch der Anorganischen Chemie, **Pd(65),** Teil 2, 328, Verlag Chemie, Berlin 1942.
[19] E. R. Andrew, Phys. Rev. **91,** 425 (1953).
[20] C. W. Fryer and J. A. S. Smith, J. Chem. Soc. (A) **1970,** 1029.
[21] Y. Ito, T. Asaji, R. Ikeda, and D. Nakamura, Ber. Bunsenges. Phys. Chem. **92,** 885 (1988).
[22] L. Latanowicz and Z. Pajak, Ber. Bunsenges. Phys. Chem. **93,** 1440 (1989).